Cellulose (2017) 24:1463–1481
DOI 10.1007/s10570-016-1181-x

ORIGINAL PAPER

Micro nanofibrillated cellulose (MNFC) gel dewatering induced at ultralow-shear in presence of added colloidally-unstable particles

Katarina Dimic-Misic · Thad Maloney · Guodong Liu · Patrick Gane

Received: 7 June 2016 / Accepted: 21 December 2016 / Published online: 10 January 2017

Abstract Aqueous nanogels are notoriously difficult to dewater. An example of such a gel is that of a suspension of micro nanofibrillated cellulose, in which water is both bound to the fibrillar surface and held within the interfibril matrix. We demonstrate a phenomenon in which dewatering of nanocellulose based gel-like suspensions can be induced by adding a colloidal particulate component, which itself can undergo autoflocculation when suspended in water. The mechanism is exemplified by the addition of undispersed precipitated calcium carbonate, which in equilibrium remains stabilised in the gel, but when the gel mix is exposed to *ultralow* shear, acting below the yield stress, demixing of the combination between the nanofibrils and the autoflocculating pigment leads to separation of the unbound water phase. This novel mechanism is proposed to enhance the dewatering capability in general of complex gel-like water-holding suspensions.

K. Dimic-Misic (✉) · T. Maloney · G. Liu · P. Gane
Department of Bioproducts and Biosystems, School of Chemical Technology, Aalto University (Aalto), 00076 Helsinki, Finland
e-mail: katarina.dimic.misic@aalto.fi

G. Liu
College of Light Industry and Energy, Shaanxi University of Science and Technology, Xi'an 710021, China

P. Gane
Omya International AG, Baslerstrasse 42, 4665 Oftringen, Switzerland

Keywords Micro nanofibrillated cellulose · Ultralow shear dewatering · De-mixing of solids in gel · Phase separation in gels · Autoflocculation

Introduction

Sustainability is a priority in modern industrial practice, and development of novel biobased composite materials, which are based on renewable sources, is considered highly relevant. Nanofibrillated (NFC) and microfibrillated (MFC) cellulose have chemo-mechanical properties such as high specific surface area, internal structural crystallinity and reactive hydroxyl groups on their surface that support a variety of chemical modifications (Klemm et al. 2011), making them interesting materials for many industrial applications, especially in the field of nanocomposites. MFC can be produced mechanically by refining of wood fibres, for example using an homogeniser, microfluidiser, refiners etc., yielding nanofibrils with broad size distribution (typical diameter of 50–100 nm) and with relatively low anionic charge (Pääkkö et al. 2008; Osong et al. 2015). Such mechanical processes involving homogenisers involve large energy consumption and are, therefore, often considered industrially uneconomic to apply in the market (Klemm et al. 2011; Spence et al. 2011) due to the high cost of the end product. Application of chemical methods prior to mechanical treatments,

such as carboxymethylation (Wågberg et al. 2008), enzymatic pretreatment (Henriksson et al. 2007; Pääkkö et al. 2008), grafting (Habibi 2014) and TEMPO oxidation (Saito et al. 2006) reduce energy consumption drastically, resulting in an end product which is nanofibrillated (NFC) with more uniform size distribution and highly anionically charged due to the breakdown of the cellulose crystalline links that releases the medium of hemicellulose trapped within the multicrystallite array. Enzymatic pretreatment of pulp prior to refining is, in particular, widely investigated due to the lowering of chemical consumption, together with limited mechanical energy input, delivering an end product, which is, in respect to surface properties and morphology, in between MFC and NFC. The enzymatic degradation acts to shorten fibrils, thus additionally aiding mechanical treatment by reducing problems related to the clogging of refiners and associated agglomeration of long MFC fibrils.

Due to the abovementioned increased research in processing utilising mechanical breakdown of fibres, with and without chemical pretreatments, a wide range of diverse materials can be obtained containing a major fraction of micro-sized entities which have nanofibrils branching from their surfaces. Such material has been conveniently termed micro nanofibrillated cellulose (MNFC) (Schenker et al. 2015, 2016). Differences in pretreatment results in MNFC systems with different surface charge and aspect ratio, such that colloidal interactions, in particular the level of agglomeration and/or flocculation within the fibrillar matrix, generate very different rheological and dewatering behaviour. Controlling these properties is critically important for applications of MNFC in the complex suspensions used for the production of nanocomposites containing a high level of mineral and other filler(s), as they have a strong impact on processability (Dimic-Misic et al. 2013a, b, 2016).

Due to the high surface area of MNFC, associated with the nanofibrillar fraction, and its respective potential for hydrogen bonding, filler loading can be drastically increased when utilised in high consistency composite materials (up to 70% filler) whilst maintaining overall strength properties. In the paper and board industry, for example, this afforded ability to add high levels of filler has a strong positive impact on optical and mechanical properties (Pääkkö et al. 2008 Klemm et al. 2011).

Hydrophilic MNFC provides high water absorbency, and, due to the high osmotic pressure within the system, both bound water on the fibril surface and clustered interstitial unbound water are present within the suspension, creating a gel-like material in suspension even at very low consistency (Nazari et al. 2013; Puisto et al. 2012). However, precisely due to their gelation properties, the main problems arising in the processability of high consistency MNFC suspensions are related to the difficulty of dewatering the product (Dimic-Misic et al. 2013a, b). In order to avoid chemically induced routes for breaking the gel structures, solutions utilising rheological behaviour have been offered that rely on the strong shear thinning properties of MNFC suspensions, such that, through reduction of viscosity and breakage of gel clusters and flocs, the suspension can be brought into usable flow. In order to tune the rheological behaviour of such systems to enhance their processability, it is therefore necessary to understand both their viscoelastic and flow behaviour in terms of fibril surface charge and morphology. The rheological characterisation of MNFC-based systems is complicated due to the diverse properties resulting from their fibrillar colloidal components, with non-linear flow curves displaying thixotropy and a difficult to define yield stress that, in turn, depends on gelation and flocculation (surface charge) and agglomeration (aspect ratio), i.e. their colloidal stability (Saarikoski et al. 2012; Naderi and Lindström 2014; Fall et al. 2011). Avoiding apparent wall-slip, or more precisely solids depletion at the sample-wall interface, in such systems requires use of profiled surfaces or specific measuring geometry, e.g. serrated surface in plate–plate geometry, and vane-in-cup spindle in cylindrical geometry (Mohtaschemi et al. 2014; Nechyporchuk et al. 2016; Haavisto et al. 2014). During rheological measurements complicating interparticle interactions in the system are accompanied with those at the particle-geometry interfaces, inducing further instrumental limitations (Naderi and Lindström 2015). Although vane spindle in cup geometry decreases the effect of apparent wall-slip, shear banding that is present between regions of different stress, due to the thixotropic nature of such systems, leads to the formation of intra-structural regions of different viscosity and thus flow properties. Considering the highly crystalline nature of the fundamental elements in MNFC, these internal structural regions act as a precursor for aligned planar

structures (Martoïa et al. 2015; Nechyporchuk et al. 2014; Nazari et al. 2016).

Rheological investigations of MNFC systems have generally followed the classical demand for industrial applications, i.e. low to high shear viscosity and structure recovery, which suits, for example, the paper and board industry. However, for some applications extended low shear conditions are necessary where it is favourable that the gel properties are preserved. For these applications, where applied stress is necessarily below the yield stress, any required dewatering must occur within the initially linear viscoelastic region (LVE). In our previous work, it was observed that mineral pigment can flow under moderate shear through a fibrillar MNFC gellant without fibril-pigment interference within the gel structure (Dimic-Misic et al. 2013b, 2015b). However, without shearing, the pigment is held in the interfibril voids within the gel once left to rest after mixing. In contrast to the case of the classical DLVO condition, where a stabilised dispersion must be destabilised by some external agent, in this case non-stabilised colloidal particles can be held in dispersed suspension by containing the particles within the trapped water associated with the gel (Dimic-Misic et al. 2015a; Fall et al. 2011).

In industrial practice both sedimentation and filtration are regularly used for dewatering of high consistency suspensions (Tiller et al. 1987; Roussel and Lanos 2004). In mineral and sludge dewatering, for example, flocculation is used as a pretreatment, where separation of the solid and liquid phase is initiated by formation of large flocs (Dentel et al. 2000; Unno et al. 1991). Hence, flocculation, mechanically or chemically induced, has to be carefully controlled so as to define the quality of a given dewatering system and, hence, the end product properties (Mikkelsen et al. 2002; Serra and Casamitjana 1998).

Flocculation is a complex process that is induced by creating conditions initially removed from equilibrium dispersion, and it is usually achieved with chemicals which act to coagulate or flocculate, depending on their nature, requiring addition and mixing control (Chaari et al. 2003). The aggregation of the fine sol particles into larger more or less loosely formed units, termed flocs, is defined by the three steps of destabilisation of the suspended fine sol particles, the first being fragmentation and growth of flocs, which is followed by increase of flocs due to adhesion and collisions within the system, and the third phase is degradation of flocs when placed under shear and/or turbulence (Serra and Casamitjana 1998; Roussel and Lanos 2004).

In paper making, filler induced flocculation within pulp suspensions is used to enhance the structural properties of paper and board, increasing light scattering, while also flocculating the filler leads to favourable properties of paper strength (Spicer et al. 1998; Hogg 2000). In the case of autoflocculation, the formation of the flocs occurs between particles of the same species due to the removal or non-existence of any form of stabilisation, which itself could have been either colloidal or, for example, incorporation with a gellant. The well-known destabilisation of Coulombic repulsion by increasing ionic strength, thereby compressing the adsorbed double layer, is one example under which autoflocculation may occur (Horvath and Lindström 2007; Fall et al. 2011; Dimic-Misic et al. 2015a). Mechanical mixing at medium to high shear, however, as mentioned above, prevents the ultimate effectiveness of flocculation (Karppinen et al. 2011; Saarikoski et al. 2012; Tsai et al. 1987). Therefore, of novel interest here is that the application of *ultralow* shear over extended timescale is seen to induce demixing of colloidal mineral particles from the gel matrix as a result of the particulate passage of the mineral through and within the gel. This occurs in the exemplified case here, namely amongst short, enzymatically pretreated MNFC fibrils and non-dispersed mineral pigment, and is related to the initial freedom of movement by such pigment (Dimic-Misic et al. 2015b, 2016). Over prolonged time under *ultralow* shear, i.e. with stress below the yield point, we hypothesise that colloidally unstable filler particles will encounter highly charge nanofibrillar material, become adsorbed and then promote flocs, i.e. autoflocculate while attached to fibrils. This behaviour, accompanied with likely shear banding within the gel suspension, is expected to lead to boundaries between the band regions (Nazari et al. 2016; Mohtaschemi et al. 2014; Nechyporchuk et al. 2014).

The scope of this research tests the hypothesis that demixing from the liquid phase and autoflocculation can lead to structuration and ultimate dewatering by studying in depth the long time-scale *ultralow* shear-induced behaviour of a filler containing MNFC gel-like system in order to propose ways in which these colloid-fibril nanocomposites can be more efficiently dewatered.

Experimental

Background

The rheology of MNFC-filler particle suspensions is known to be dependent on the surface charge and morphology of fibrillated cellulose, associated with the state of gelation and flocculation (Pääkkö et al. 2008; Horvath and Lindström 2007; Puisto et al. 2012). Complex rheological behaviour of such suspensions is related to the mobility and friction between the fibril–fibril and filler-fibril matrix, which depends on the swelling of fibrils, flocculation-related destabilisation and entanglement (Dimic-Misic et al. 2013b, 2015b). Not only under flow conditions but also under low/*ultra*low shear conditions gel-like MNFC structure additionally is influenced by the volume fraction ratio of the different constituents within the suspension (Fall et al. 2011; Nazari et al. 2013).

Calcium carbonate is known to dissociate in its virgin form in water into Ca^{2+} together with the release of CO_2 and some formation of hydrogen carbonate and carbonic acid in equilibrium. In respect to charge stabilised colloidal materials, an increase in ionic concentration acts to screen the charge and to shrink the double layer. For freely mobile particles this then leads to flocculation. There is, however, a strong distinction between freely mobile colloidal particles and those locally immobilised in a gel matrix structure, i.e. the MNFC fibrils are networked in a way which entraps gel water in the static state, as well as having water adsorbed and immobilised onto their surfaces, predominantly by hydrogen bonding. In earlier work we showed that filler particles are able to pass without interaction with the fibrils when the sample is sheared beyond its yield point, indicating little to no attraction potential between the species. The Ca^{2+} ion is itself, therefore, not the acting factor in generating a state of flocculation-driven dewatering, since, as we shall see, there is no effect whether the sample is either not sheared (mixed MNFC and filler and then left static) or sheared above the yield point over time, and again then allowed to stand undisturbed. Only the application of *ultralow* shear will be shown to enable the function of the calcium carbonate in respect to its impact on MNFC fibrils in acting to expel gel water and promote the formation of a fibrillar structure. We aim, therefore, to test convincingly that the ionic concentration generated by adding calcium carbonate particles *per se* does not alone lead to the strong flocculation of the fibrils required to cause dewatering by charge screening, otherwise the unique action of applying *ultralow* shear would be redundant. At this point of publication, without further detailed work, it is premature to attempt to enlarge on hypothetical mechanisms other than to say that the requirement of controlled *ultralow* shear to induce the structuring effect suggests competitive rates of interaction via enforced long timescale contact versus either diffusion or particle flow. Additionally, the action of the calcium carbonate is seen to be related to its own ability to undergo autoflocculation. This is confirmed by considering the comparison with polyacrylate dispersed calcium carbonate, the action of which is to provide anionic stabilising charge to the pigment particles, which, in this case, will be shown to prevent any interaction with the similarly charged fibrils under any conditions of applied shear.

In this analysis we firstly use viscoelastic measurements inside the linear viscoelastic region (LVE), prior to testing the dewatering condition proposed, to characterise the samples in respect to micro structure, thus also avoiding wall depletion effects which arise during steady state measurements. We then secondly proceed with rheological measurements in order to capture the effect of shear below the yield point and shear thinning region, by applying constant *ultralow* shear rate for a prolonged period of time, inducing the proposed autoflocculation of non-dispersed versus dispersed pigment, observed via the change in dynamic viscosity (η). In the final part we link the rheological properties with optical images to capture visually the suspected solid–liquid phase separation caused rheologically by the pigment–pigment to fibril autoflocculation process. To provide a practical aspect for the application we include a study of both the starting fibre source for the enzymatic pretreatment of the MNFC, and a furnish-like blend of MNFC and pigment.

Materials and methods

Bleached never dried hardwood Kraft pulp (BHW), obtained from a Finnish pulp mill, with an average fibre length of 1.23 mm measured with a FiberLab analyser (Metso Automation) was used for the preparation of MNFC. This same pulp was used in two roles, the first as the fibre content in a furnish-like filler-free

formulation, and secondly in the production of the MNFC itself using enzymatic pretreatment in the process described in detail by Rantanen et al. (2015). In brief, pulp was washed to the sodium form with a 2 wt% of sodium hydroxide solution until the pH 10, and then washed with deionised water with a conductivity of 8.2 µS. For enzymatic pretreatment the cellulase enzyme containing ECOPULP® R (cellulase activity 84 000 $CMUg^{-1}$ determined on CMC-substrate at 60 °C and pH 4.8, as described by supplier) was applied at 3 mg of enzyme per gram of pulp fibres in a 2.5 wt% pulp suspension. During hydrolysis, the suspension of pulp and enzyme was agitated at a temperature of 57 °C and pH 5.5, for 2 h, using hydrogen chlorite as a buffer. By increasing pH to 9–10 with sodium carbonate and raising the temperature to 90 °C the enzymatic degradation were terminated. The resulting suspension was placed in a cold storage to cool overnight and then refined in a Valley Hollander for 30 min and subsequently fed two times through a microfluidiser (model M-110P, Microfluidics, USA) in order to obtain MNFC with favourable particle size and morphology. The pressure in the fluidiser was controlled at 2 000 bar and the flow gap set to 100 µm. The solids content of the MNFC obtained was 1.65 wt% (Dimic-Misic et al. 2016).

The freely added filler, for comparison with unfilled samples during shearing, was a precipitated calcium carbonate (PCC) commercial grade having scalenohedral morphology (Syncarb FS-240 from Omya International AG, Switzerland). It was delivered as a water suspension at 35 wt%, essentially dispersant-free polysaccharide stabilised against sedimentation. In order to capture the role of the autoflocculation (self-flocculation) effect of non-dispersed pigment during demixing from the MNFC-water matrix, alternatively, by way of a control, 0.01% of sodium polyacrylate dispersing agent was used to form a sample of dispersed pigment. Both non-dispersed and dispersed pigment were used for preparation of the respective samples, as described in the following section and shown in Table 1.

Sample mixes

A matrix of samples was produced to match a desirable high filler load that might be used in MNFC based paper and board manufacture, but which is also considered as a realistic sustainable polymer composite replacement, in constant total solids fractions in aqueous suspension at different consistencies. Using these samples it is possible to determine low shear agglomeration phenomena and further on to observe the phase separation of the differentially flocculated material following the formulation principles described in earlier work (Klemm et al. 2011; Dimic-Misic et al. 2015a, b). Sample consistency was increased by centrifugation from the initial suspensions where needed, and subsequent dilutions from the concentrated stock were made using deionised water.

The sample labels follow the notation as presented in Table 1, with the composition ratio of the component samples held constant with 70 wt% filler in total. The samples were made down into three different consistencies, 3, 5 and 10 wt%, following constant solids fractions in suspensions as presented in Table 2.

Materials characterisation

Zeta potential, particle and agglomerate size

To help characterise the constituents of the coatings, a Zetasizer (Malvern Instruments Ltd., UK) was used to determine electrophoretic mobility to evaluate the zeta potential, ζ, of the pigments and the MNFC material and Mastersizer 2000 (Malvern Instruments Ltd., UK) was used to determine the particle size of the PCC pigments and agglomerate size of MNFC by static light scattering. Prior to measuring the ensemble defined particle size, the samples were diluted with deionised water to a solid content of 0.01 wt%. The volume median diameter ($d_{sv}(0.5)$ and zeta potential (ζ) are reported as an average of at least five runs, and are reported in Table 3. The length-weighted average length of the pulp fibres were determined using a Metso FiberLab image analyser (Kajaani FiberLab TM, Metso Automation, Finland) (Liimatainen et al. 2013). Diluted pulp suspension (0.004 wt%) was placed into the sample unit and the length measurement laser optics detects the presence of a fibre and monitors its passage through the capillary. Each sample was analysed in triplicate.

Water uptake of samples; gravimetric dewatering and water retention value (WRV) measurements

Both water retention (WRV) measurements and gravimetric dewatering under pressure, as used to define

Table 1 Sample formulations used in the study

Additionally, the pigment is used either in undispersed sor dispersed form both for samples containing pigment suspension alone and in the case of the mixed MNFC-pigment systems

Formulation		Component/pph based on total weight		
		Fibre (BHW)	MNFC	PCC
F1	100			
F2		100		
F3_d. F3_u.d.	Dispersed PCC			100 dispersed
	Undispersed PCC			100 undispersed
F4_d. F4_u.d.	MNFC + dispersed PCC		30	70 dispersed
	MNFC + undispersed PCC		30	70 undispersed

Table 2 Sample formulations prepared to preserve constant component fractions between constituents, while containing the required amount of each component in parts per hundred (pph)

Samples were prepared to match at three different concentrations 3, 5 and 10 wt%. Amount of each component in the samples was calculated in each case, respectively

Sample (from Table 1) /designed at 3, 5 and 10 wt% consistency, respectively/	Density (g cm^{-3})	Measured solids content (%wt)
F1/3	1.015	3.00
F2/3	1.015	3.00
F3/3	1.051	2.90
F4/3	1.040	2.93
F1/5	1.025	5.00
F2/5	1.025	5.00
F3/5	1.086	4.74
F4/5	1.067	4.81
F1/10	1.050	10.00
F2/10	1.050	10.00
F3/10	1.171	9.10
F4/10	1.135	9.34

Table 3 Properties of materials used in this study: network swelling-related WRV, surface charge as zeta potential (ζ), pH and volume MNFC and PCC median particle size (d_{SV} (0.5)

Material	WRV (g g^{-1})	ζ (mV)	pH	d_{sv} (0.5) (μm)
Pulp (SR 24)	1.5	−18.4	6.8	99.4
MNFC	2.8	−26.1	6.7	43.7
Dispersed PCC	N.A	−10.6	10.3	4.5
Undispersed PCC	N.A	+0.5	10.3	7.8

SR refers to the Schopper-Riegler value of the fibre pulp

water holding properties of suspensions, were slightly modified to suite gel-like MNFC suspensions, as described in detail by Dimic-Misic (2013a, b). Briefly, the water uptake of cellulosic materials was evaluated (WRV ISO/DIS 23714) by centrifuging mixtures of different quantities of the MNFC with unrefined Kraft pulp and extrapolating the WRV values against different MNFC contents used to determine the water content of the pure MNFC component. Gravimetric dewatering of suspensions was measured using the Åbo Akademi Gravimetric Water Retention device (ÅA-GWR). An average of five determinations was computed for both the WRV and ÅA-GWR tests with data variation found to be within 10%.

Rheometry

Since MNFC suspensions are gel-like and thixotropic, and prone to apparent wall slip related to solids depletion at the sample-wall interface. Experimental observations using only smooth wall geometry suggest that the nanocellulosic gel-like suspension rotates mostly as a plug/block, with the shear occurring at or near the smooth boundary (Martoïa et al. 2015; Nechyporchuk et al. 2014). The results from previous research points towards a water layer formation near the stator, and slow breakdown of the network or gel structure throughout the material upon reaching a yield point, to explain the shear-thinning mechanism (Dimic-Misic et al. 2015b).

Due to the complex nature of flow curves and their thixotropic character, fitting the steady state data to an Herschel-Bulkley yield stress model, as is usually used for nanocellulosic materials, can result in the misconception in respect to the obtained dynamic yield stress (τ_s^o) values (Mohtaschemi et al. 2014). Therefore, the rheological effect of the physical and colloidal interaction within the sample matrices consisting of solid constituents is investigated with oscillatory measurements, where rheology of the samples is studied without breaking down the microstructure in the gel-like system (Nazari et al. 2013, 2016), thus minimising the effect of apparent wall slip/depletion. All rheological measurements were obtained with a controlled strain rheometer (Anton Paar Physica MCR-300).

For the oscillatory viscoelastic measurements a smooth plate–plate geometry was used for filler suspensions and serrated plate–plate geometry with the profile on both upper and lower plate for fibrillar samples; diameter of upper plate was 20 mm, and the plate was connected with a Peltier temperature control, set to a constant temperature of 23 °C. The gap was initialised to 2.3 mm for Kraft pulp suspensions, 1.5 mm for MNFC suspensions (due to the height scale of the serrated surface) and 1 mm for filler suspensions. Gap changes were adjusted to correspond with the particulate size of the samples in respect to the smooth/profiled geometry. This latter adjustment avoids solids depletion layers in the case of filler suspensions, and allows for the presence of larger fibrillar material in the samples ranging from MNFC to pulp (Dimic-Misic et al. 2013a, 2015a; Saarinen et al. 2009). All suspensions were measured applying a strain sweep with strain (γ) in the range varied between 0.1 and 500%, and constant angular frequency (ω) of 10 (rad) s^{-1} to determine the linear viscoelastic region (LVE). For the following corresponding frequency sweep measurements, a constant strain of $\gamma = 0.1\%$ in the linear viscoelastic (LVE) region was used with ω spanning the range of 0.01–100 (rad) s^{-1}. Prior to the oscillatory measurements, the samples were presheared to provide a relatively slow mixing at a shear rate of $\dot{\gamma} = 10\,s^{-1}$ for 60 s and then left to rest for a further 60 s.

Oscillatory measurements were also used for determination of the apparent yield stress, which we previously defined as static yield point, τ_s^0 (Dalpke and Kerekes 2005; Dimic-Misic et al. 2016). The static stress component (τ_s^0) is described by

$$\tau_s^0 = G'\gamma_c \quad (1)$$

During the strain sweep measurements, the elastic modulus G' is recorded as γ increases, and the maximum static stress at the critical strain γ_c is taken to correspond to the static yield stress τ_s^0, and is determined as the first point of deviation from the linear stress (τ_s)-strain (γ) curve occurring at the critical strain γ_c (Horvath and Lindström 2007).

Dynamic viscosity–vane rheometry

In order to follow the behaviour of colloidal non-stable filler flocculation and structuration within the gel-like MNFC suspension, it is necessary to avoid floc rupture, which normally arises under dynamic shear conditions. Therefore, following initial pre-shearing and allowing to relax, *ultralow* shear was applied at shear rate $\gamma. = 0.01\ s^{-1}$, which was within the re-established LVE. Low shear rate structure analysis and the study under *ultralow* shear rate were performed with a bob in cup geometry where the "bob" was a four bladed vane spindle with a diameter of 10 mm and a length of 8.8 mm, while the metal cup had a diameter of 17 mm (Anton Paar, Germany).

Visual observation and nitrogen cryo-fixation

The samples were studied optically in situ in the rheometer by replacing the metal cup with a glass container having the same diameter as the bob geometry.

To capture the different phases of the rheologically controlled mechanism of gel water and pigment demixing in more detail, two sets of samples were prepared for freeze drying: namely, with and without *ultralow* shear applied for a duration of 10 min. To enable this freeze drying study to be made, the rheological measurements were again replicated by inserting a suspension into a similarly dimensioned plastic vessel. Liquid nitrogen has a boiling point of −186 °C, and samples in plastic cylinders were dipped into liquid nitrogen for 5 min, being previously found to be an optimal time for freezing the total volume of the sample. After freezing, samples were left for 24 h in a freeze dryer at −50 °C and 2.4 bar and after sublimation low density aerogels were obtained.

Microscopy

Optical microscopy was used to study both the fibrillar sample suspensions and aerogels using an Olympus BX 61 microscope equipped with a ColorView 12 camera. A stereo optical microscopy imaging was used to investigate the pore and overall size structure of the freeze dried samples in aerogel form after the rheological shear treatment.

Scanning electron microscopy (SEM) imaging from aerogel samples employed a thin layer of gold coating and then placed into a field emission scanning electron microscope (FE-SEM, Zeiss Sigma) with an accelerating voltage of 2.5 kV.

Reproducibility

For pigment dispersions, data variation of the static water retention ÅA-GWR and rheometrical measurements for filler suspensions were within ±5%, while for samples containing pulp or MNFC within 10% due to the nature of the particle size-sensitive gel structure. For measurements in the vane-in-cup geometry and plate–plate geometry there is also the presence of shear inhomogeneities contributing to reduced reproducibility. Data noise was removed with the Tikhonov regularisation smoothing method modified to suite complex rheological systems, as described in detail in our previous work using a similar approach (Dimic-Misic et al. 2014).

Results

Material properties

Differences in the degree of dispersion versus aggregation of pigment particles when adding polyacrylate dispersant to the PCC pigment suspension, obtained with light scattering, are evident in Fig. 1a. Undispersed pigment particles have a trimodal size distribution with somewhat larger agglomerate size than the dispersed pigment suspension, which itself is bimodal, indicating the scalenohodral aggregate structure versus the single particulate PCC crystal component.

Enzymatic pretreatment accompanied with refining leads to the decrease in fibril size, (Fig. 1a–d), where hardwood fibres analysed with FiberLab are in the millimetre range, (Fig. 1b), while MNFC aggregates are in the micrometre range, analysed with light scattering, (Fig. 1a). These results show that the decrease in fibril size should act to reflect an increase in surface area of the fibrils, and the resulting colloidal networking trapping more water in the gel forming mechanism, as presented in Table 3.

The properties of the materials in respect to fibril water retention value (WRV), zeta potential (ζ), pH and volume median size ($d$sv(0.5)) are shown in Table 3. Enzymatic pretreatment of Kraft pulp prior to fluidisation acts to create a water arresting fibrillar network, due to the drastic decrease in fibril size and increase in their surface area coupled with the increase of surface anionic charge, due to the presence of hemicellulose, which is revealed through WRV results (Dimic-Misic et al. 2013a).

Rheology

Viscoelasticity

Due to the high level of gellation MNFC in the suspension, when adding a high amount of filler component in the system ensuring a good dispersion of filler within the high aspect ratio MNFC matrix, which has gel-like properties, is critical. The viscoelastic properties of the single constituents, MNFC and respective fillers, have been found to affect in turn the viscoelasticity of the mixed suspension (Dimic-Misic et al. 2013b). The response of upon addition of inert filler to highly flocculated fibre systems, such as

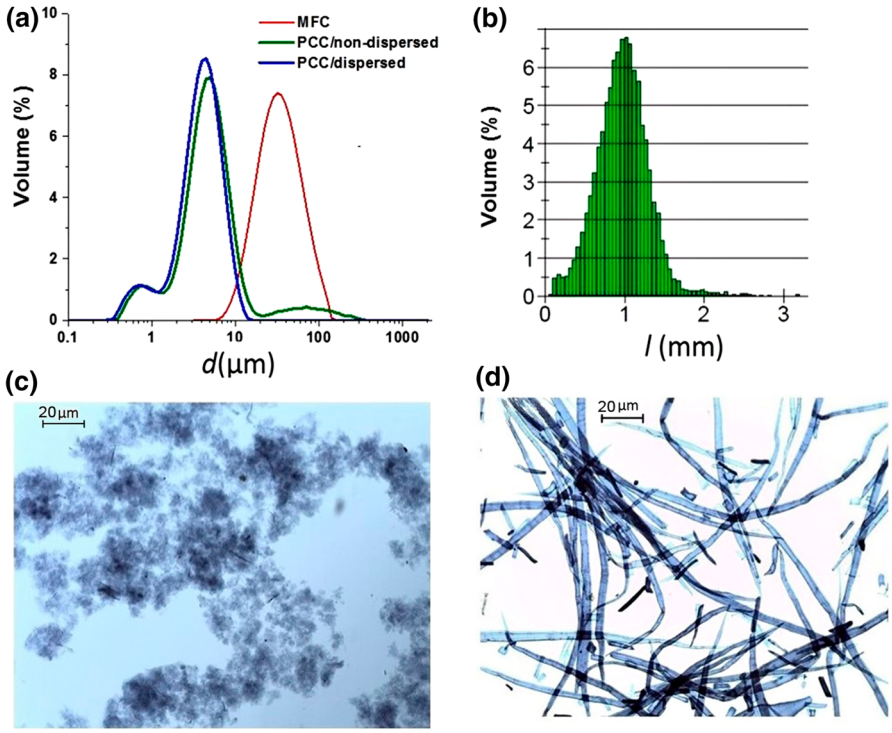

Fig. 1 Size distribution of MNFC and PCC: **a** change from tri-modal to bi-modal size distribution upon dispersion of PCC when flocculation is eliminated. The size distribution of MNFC obtained with light scattering is monomodal. **b** The pulp fibre size distribution obtained with FiberLab showing the length of starting material, from which **c** the MNFC is derived. The original kraft fibre structure microscopic image is additionally shown in **d**

pulp fibres, versus more stabilised MNFC fibrils is observed through the change of agglomeration and entanglement in the system, and its effect on the viscoelastic properties and yield point of the suspension (Dimic-Misic et al. 2016). Shorter fibrillar material MNFC (Fig. 1a–c), where the measurement is made under highly diluted conditions, has correspondingly lower level of static network strength than at higher solids concentration, and, thus, lower elastic (G') and viscous (G'') moduli, (Fig. 2b), than the long fibre pulp suspension, (Fig. 2a), indicating lower network strength for short MNFC fibrils and higher viscoelasticity of flocculated/entangled long pulp fibres (Mohtaschemi et al. 2014). MNFC, however, shows an increase in viscoelasticity when consistency is increased, seen through the increase in magnitude of both G' and G'', and the appearance of a critical strain γ_c, leading to structure yield, for 5 and 10% consistency, respectively, which is absent for the pulp suspension.

Oscillatory measurements of dispersed and undispersed filler suspensions, Fig. 2c, show that colloidal stabilisation of the filler results in G' having a more uniform dependence on strain, due to the absence of flocculation. Moduli are consistency dependent, and, for 5 and 10% consistency, the flocculated sample of undispersed pigment shows a crossover of moduli, i.e. viscoelastic behaviour, but for the low 3% consistency sample G'' is higher than G' throughout the whole strain interval, indicating strong viscous fluid-like behaviour.

Introduction of filler into the gel-like MNFC (F4) shows the typical strain hardening behaviour of the loss moduli (G'') when filler is in the undispersed form, characterised by an overshoot in the G'' curve for higher strains, Fig. 2b, already indicating some autonomous interaction between the undispersed filler particles (Dimic-Misic et al. 2015a). This G'' increase after the critical strain associated with initial yield, γ_c, is typical for gel systems that have in their matrix fillers and can indicate interactions between the components, i.e. weak adsorption and/or autoflocculation.

As observed previously for MNFC gel-like systems, G' and G'' are seen to be almost independent of angular frequency (ω), showing that oscillation frequency does not induce elastic structure, which, on the contrary, generally does happen for much higher

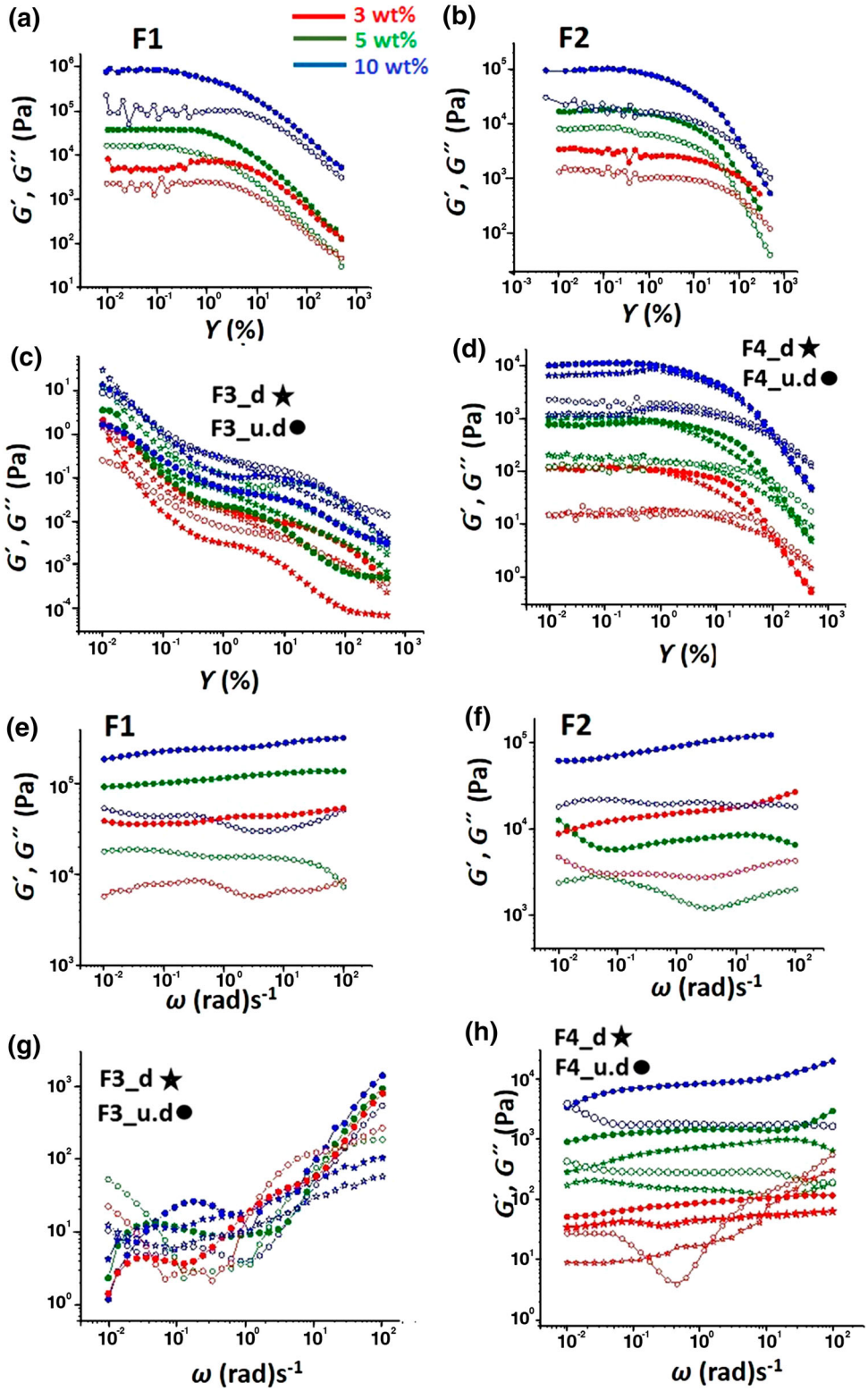
(a)
F1
3 wt%
5 wt%
10 wt%
G′, G″ (Pa)
Y (%)
(b)
F2
G′, G″ (Pa)
Y (%)
(c)
F3_d ★
F3_u.d●
G′, G″ (Pa)
Y (%)
(d)
F4_d★
F4_u.d●
G′, G″ (Pa)
Y (%)
(e)
F1
G′, G″ (Pa)
ω (rad)s-1
(f)
F2
G′, G″ (Pa)
ω (rad)s-1
(g)
F3_d ★
F3_u.d●
ω (rad)s-1
(h)
F4_d★
F4_u.d●
G′, G″ (Pa)
ω (rad)s-1

◀**Fig. 2** Elastic (G') and loss (G'') moduli dependence on strain (γ) for single component samples (**a**–**d**) where: **a** F1, **b** F2, **c** F3 undispersed and dispersed filler suspension and **d** F4 MNFC and dispersed and undispersed filler, respectively. Data from frequency sweep measurements reveal elastic (G') and loss (G'') moduli angular frequency (ω) dependence in **e**–**h** where: **e** F1, **f** F2, **g** F3_d. and F4_u.d., **h** F4_d. and F4_u.d. Dispersed *filler* samples (F3_d. and F4_d.) are presented with *star symbols*. *Closed symbols* present elastic moduli and *open symbols* loss moduli

consistency solids suspensions (Naderi and Lindström 2014; Nazari et al. 2016). Typically, upon addition of other components, the G' is expected to depend on the solids concentration and the interactions between all the components. A decrease in magnitude of both G' and G'' when the system changes from long flocculated pulp fibres, (Fig. 2c), to short gel-like MNFC is seen in Fig. 2d, and can be explained, as to be expected, with the decrease in floc size and friction within the sample.

The data in Fig. 2f, h show correspondent angular frequency dependent behaviour of G' and G'', as discussed in relation to Fig. 2a, b. Frequency sweep measurements for filler suspensions, Fig. 2g, show typical behaviour of carbonate suspensions, with both G' and G'' being consistency dependent and increasing at higher frequencies, which is more evident when the filler is colloidally unstable, as in the case of the undispersed pigment sample (Dimic-Misic et al. 2015a).

Additionally, the presence of a large amount of filler creates more uniformity in the suspension matrix, seen as G'' dependence on ω, and lower values of G' and G'' (F4), in Fig. 2h, than for the MNFC sample without filler pigment, (Fig. 2f), while colloidal stabilisation of the pigment even further reduces flocculation, as also seen in Fig. 2g, h.

The viscoelasticity in the matrix of the filler-fibril network changes when the system is sheared, due to the decrease in floc size, and that can be traced with angular frequency (ω) dependence of both moduli (G' and G'') and complex viscosity (η^*), which are dependent on consistency and interaction of all components within the system. Due to the shear thinning nature of flocculated suspensions, these complex suspensions follow a power law model for low ω, showing a complex viscosity (η^*) decrease as a function of increasing ω (= 0.1-100 (rad) s^{-1}) within the LVE region in Fig. 2, characterising the transition from elastic to viscous behaviour, (Fig. 2a–d). Flow curves of η^* for pure pulp and MNFC, (Fig. 2a, b), and composite suspensions, Fig. 2d, follow the power law model given as,

$$\eta^* = k^*(\dot{\gamma})^{n-1} \quad (2)$$

where k^* is the consistency or flow coefficient and n describes the shear thinning properties of the sample. MNFC shows very pronounced shear thinning behaviour, typical for nanocellulose suspensions, while the greater entanglement tendency within the pulp alone is seen through higher k^* values, (Fig. 3a) and presented in Table 4. In the case of the PCC suspensions, the response of η^* in Fig. 2c shows more uniform behaviour for the dispersed filler suspension than for undispersed, with evident absence of a power law behaviour across all three consistencies. Similarly, presence of filler in the MNFC matrix, which is either dispersed or flocculated, acts to change the nature of the flow curves, seen as deviation of the flow curve when undispersed filler flocculates in the gel-like fibrillar matrix, (Fig. 2d).

For MNFC-filler containing samples, (Fig. 3c), the inclusion of dispersed filler creates a more uniform dependence of η^* on ω, while the flocculating effect in the undispersed filler-MNFC complex during breakdown of the gel-like matrix induces slightly dilatant behaviour, which arises from possible structuring (Dimic-Misic et al. 2015a, b).

The main influences on the degree of flocculation and water binding gelation within the fibrillar suspension are consistency and degree of dispersion, which affect the static stress (τ_s) dependence on strain (γ), and, correspondingly, static yield stress (τ_s^0), (Fig. 3e–h). It is evident that higher consistency suspensions have higher values of τ_s^0 (Horvath and Lindström 2007; Dimic-Misic et al. 2016). Similarly, pigment flocs present in undispersed filler suspensions affect the elastic "strength" of their suspensions, as seen by the increase in τ_s^0 expressing the work needed to break filler aggregates, (Fig. 3h) (Dimic-Misic et al. 2015a). Additionally, as discussed in previous figures, dispersing the filler removes the aggregation, and thus acts to reduce the work needed to break the elastic structure and induce flow of the suspension, (Fig. 3g, h) and complete viscoelastic data in Table 4.

Ultralow shear phenomenon

The low shear structure build-up in microfibrillated cellulose (MFC) observed in our previous research

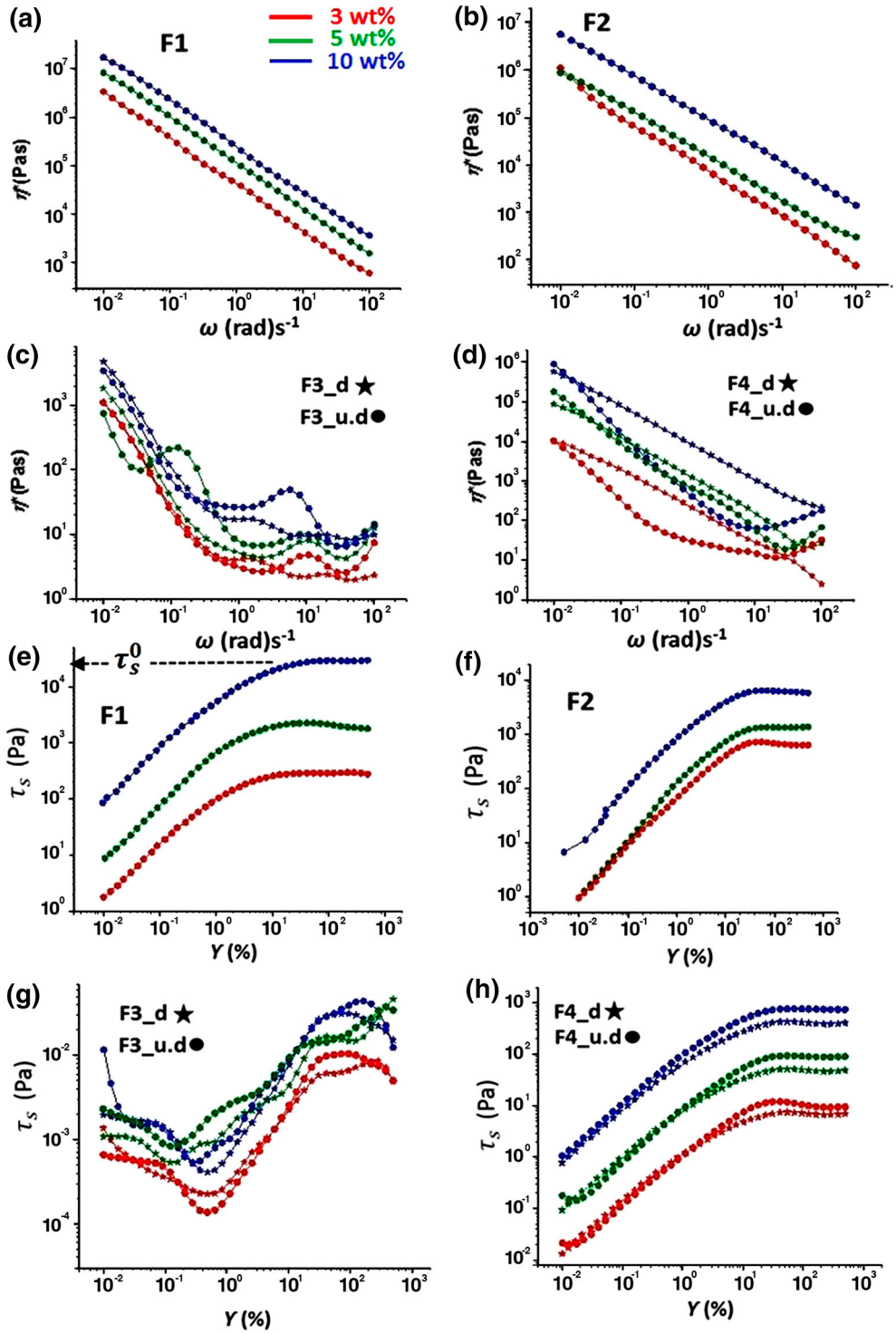

Fig. 3 Complex viscosity (η^*) as a function of angular frequency (ω): **a** F1, **b** F2, **c** F3_d. and F3_u.d., and **d** F4_d and F4_u.d., respectively. Static stress (τ_s) as a function of strain (γ), and static yield stress (τ_s^0) as a maximum of the stress–strain curve: **e** F1, **f** F2, **g** F3_d. and F3_u.d., and **h** F4_d. and F4_u.d., respectively. Dispersed filler samples (F3_d. and F4_d.) are presented with *star symbols*

Table 4 Viscoelastic parameters and gravimetric dewatering (ÅA-GWR) results for all samples: Rheological parameters obtained within linear viscoelastic region (LVE): (i) elastic moduli (G') and loss moduli (G'') taken at $\omega = 0.12$ (rad) s^{-1}, (ii) initial and final values of complex viscosity (η^*) for low and high angular frequency (ω), (iii) flow indices (k^*) and shear thinning coefficients (n), and (iv) static yield point (τ_s^0) obtained from amplitude sweep measurement

Rheological parameters	Target consistency (wt%)	F1	F2	F3_u.d.	F3_d.	F4_u.d.	F4_d.
$G'_{\omega=0.12\,(\mathrm{rad})\,s^{-1}}$ (Pa)	3	19,504	5823	5	4	55	33
	5	23,642	32,909	11	9	268	167
	10	35,246	72,641	25	22	1275	557
$G''_{\omega=0.12\,(\mathrm{rad})\,s^{-1}}$ (Pa)	3	8012	3000	4	3	40	14
	5	14,867	20,143	5	4	146	43
	10	44,456	24,270	12	7	456	283
k^*	3	11,844	7711	24	21	412	167
	5	42,731	15,447	29	26	913	234
	10	257,793	91,749	35	30	956	734
n	3	0.06	0.01	0.53	0.62	0.18	0.22
	5	0.05	0.10	0.53	0.63	0.21	0.24
	10	0.01	0.10	0.60	0.71	0.23	0.24
τ_s^0 (Pas)	3	284	127	0.05	0.03	128	90
	5	2206	721	0.07	0.05	320	219
	10	28,349	1349	0.1	0.07	763	610
Filtrate amount (ÅA-GWR) (gm^{-2})	3	8831	5661	N.A.	N.A.	2871	2671
	5	6896	3386	N.A.	N.A.	634	523
	10	3258	1750	N.A.	N.A.	424	224

(Dimic-Misic et al. 2015b), both as individual component and as a third component in a filler-pulp mix, involves longer scale mechanically-only produced fibrils compared with the enzymatically pretreated route in forming the current MNFC. Thus, the previous studies showed a self-assembly orientation mechanism at play, which was observable through viscosity increase, i.e. rheopectic structuration of suspensions under continued low to moderate shear. We see in this current work, that, additionally, structure formation can be induced independently in relation to the interactions induced by just one component present in the complex suspension, in this case a self-(auto) flocculating effect of undispersed filler, provided demixing can be induced via a likely slow rate adsorption onto nanofibrils. The dimic-misic to generate the correct demixing rather than a continuous remixing (Dalpke and Kerekes 2005; Saarikoski et al. 2012; Serra and Casamitjana 1998). Therefore, upon *ultralow* shear application over long time period, it is possible first of all to observe the change in dynamic viscosity (η) due to the long fibre entanglement, (Fig. 4a), and separately the autoflocculation effect of the undispersed filler after demixing, (Fig. 4c–d). Autoflocculation over an extended period of *ultralow* shear is the hall-mark of the undispersed PCC alone, showing long term viscosity increase, (Fig. 4c), whereas this is completely absent for the dispersed pigment, (Fig. 4d), which in turn shows a constant viscosity over time. This effect of undispersed versus dispersed filler can now be seen also for the MNFC-filler suspensions, (Fig. 4e), where the absence of rheopexy when the filler is dispersed is shown in the inset portion of the figure.

For single component fibrillar suspensions, as shown in Fig. 4a, b, it is evident that *ultralow* shear far beyond the yield point induces entanglement within the pulp suspension, which evidently after longer time reaches an equilibrium state between formation and break up, and so the viscosity reaches a steady state (Mohtaschemi et al. 2014; Dimic-Misic et al. 2015b). In contrast, a much sharper and shorter dynamic viscosity increase for the MNFC indicates a stress build within and subsequently rapid breakdown of the gel-like suspension due to the short elements in the form of the fibrillated material.

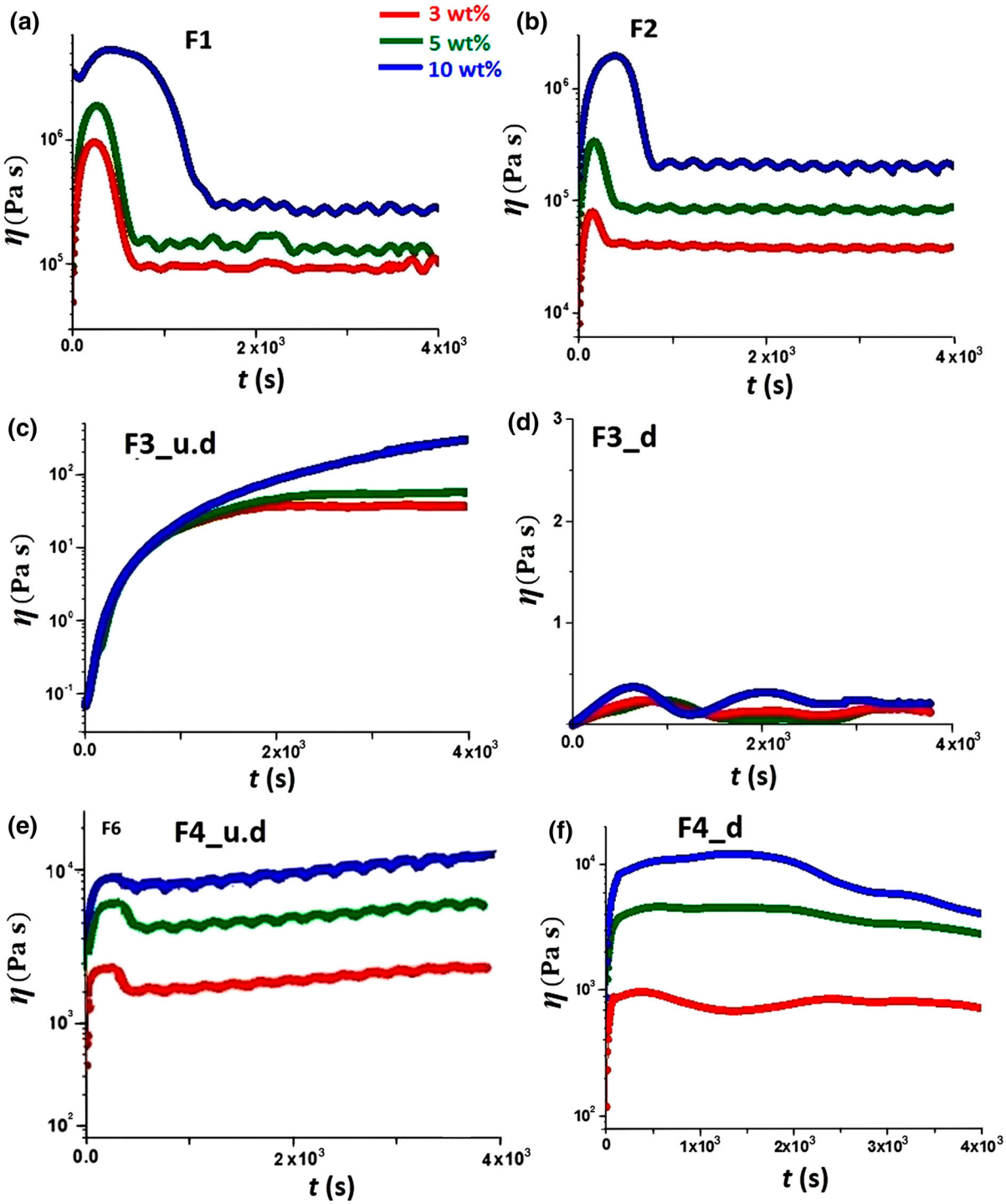

Fig. 4 Dynamic viscosity (η) dependence on time for *ultralow* constant shear rate ($\gamma. = 0.01\ s^{-1}$) for single component samples, **a** F1, **b** F2, **c** F3 undispersed filler suspension F3_u.d.), **d** F3 dispersed filler suspension (F3_d.), and **c** F4 MNFC and undispersed filler (F4_u.d.), with inset showing the stable case of MNFC with dispersed filler (F4_d.), corresponding to the behaviour in **d**

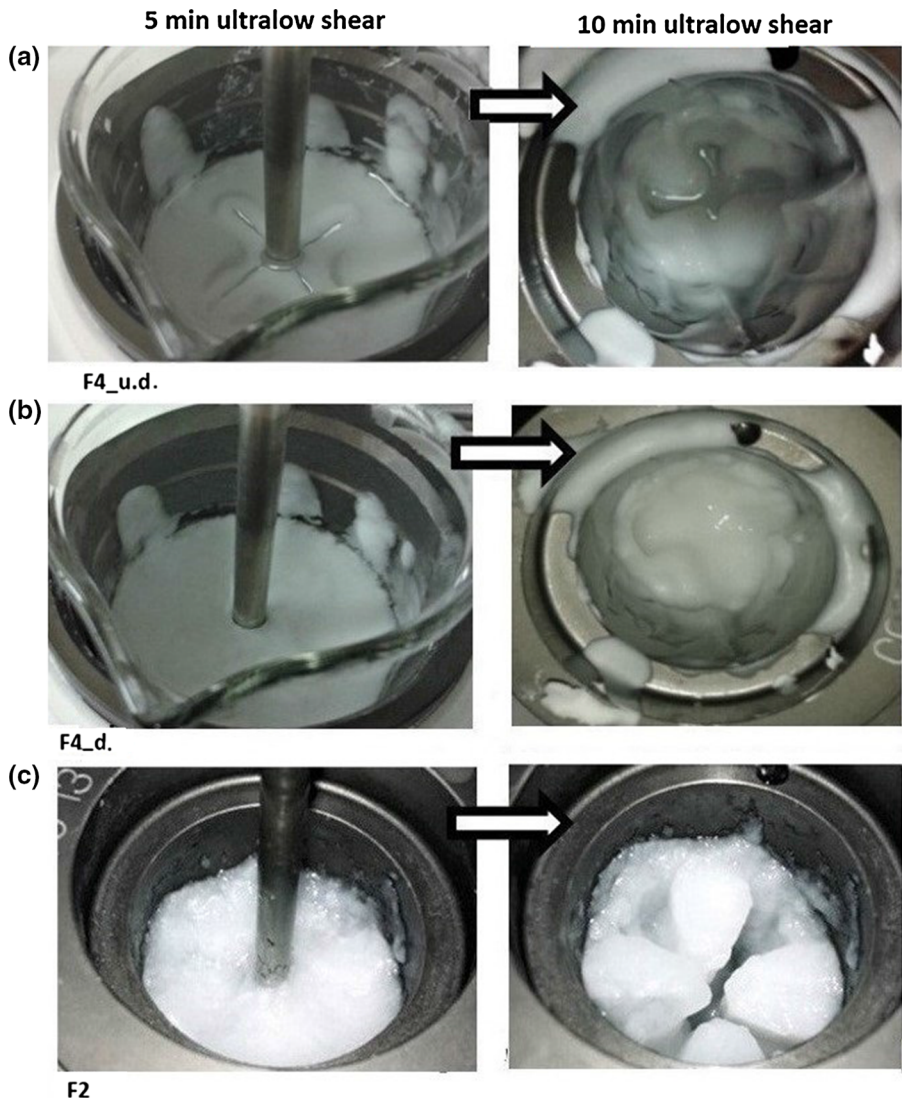

Fig. 5 Digital camera images of the samples during the ultralow shearing (0.01 s^{-1}) as a function of time, after 5 min and upon lifting the vane from the samples after 10 min of ultralow shearing; **a** F4_u.d. (undispersed filler in MNFC). The cases **b** F4_d. (dispersed filler in MNFC) and **c** F2 (MNFC) gel alone seen to remain completely intact during the measurement

To emphasise once again, however, the MNFC suspension containing undispersed filler (F4_u.d.), Figure 4e, shows structure build at *ultralow* shear, as was observed for undispersed filler alone, but the dispersed filler in MNFC (F4_d.) shows far less of this effect, as shown in the inset plot also in Fig. 4e. We may conclude, therefore, that the system containing undispersed filler is undergoing demixing and autoflocculation under *ultralow* shear, i.e. below the apparent yield stress (Serra and Casamitjana 1998). Higher shear, as we saw earlier, maintains a mixed system and so the presence of MNFC with its gellant properties prevents the flocculation of the undispersed filler—compare Fig. 4b with Fig. 4e (Dimic-Misic et al. 2013a; Spicer et al. 1998).

Induced dewatering at ultralow shear

The visible impact of the free water separation resulting from demixing and autoflocculation is shown in the photographs in Fig. 5 taken after just 5 min and after 10 min of *ultralow* shearing of the samples in the

cylindrical vane in cup geometry. The main focus here is on the demixing induced by *ultralow* shear, occurring below the apparent yield stress, followed by autoflocculation of the colloidally unstable undispersed filler, now released the gel water matrix, leading to an induced phase separation visible as a layer of liberated unbound water. This is exemplified by the case of samples F4_u.d in Fig. 5a. The control samples are the alternative F4_d., where the pigment is dispersed and so stable, presented at Fig. 5b, and MNFC alone (F2), Fig. 5c, where, in both the latter cases, no dewatering takes place and the gel remains intact. After 5 min of *ultralow* shearing, the formation of the boundary water layer is visible only in the case where the undispersed filler is present (F4_u.d.), Figure 5a shows the appearance of structured zones displaced from the vane and spindle, which become even more well-defined after 10 min. These structured zones around the vane are not present when the filler is dispersed (F4_d.), nor in the MNFC suspension alone (F2). The water is released from that portion containing the demixed and flocculated filler suspension, and is creating boundary layers between the pigment-rich areas and the remaining gel-water matrix, creating a novel opportunity to remove the water at these boundary layers with the vessel and rotor. The "pooled" water in the void volume left after removal of the vane element is clearly visible for the F4_u.d. sample in Fig. 5a, for which the demixing and autoflocculation of the filler was observed. That this water does not disappear in the remaining static sample shows that the flocculation is not solely diffusion dependent but is induced by near particle–particle contact under *ultralow* shear at a forced residence time other than that offered by diffusion alone, and slower than gel breakdown through mixing, where the pigment plays the role of flocculating agent or structuring intermediary. The mix of MNFC and dispersed filler (F4_d.), as well as the MNFC alone (F2) show no such phase separation, (Fig. 5a, b).

In order to confirm and support the proposed complex rheologically-induced *ultralow* shear demixing of autoflocculating pigment and resultant phase separation within the undispersed pigment-MNFC system, the aerogels were studied, each formed by freezing directly from sheared and non-sheared samples for comparison in the cases of both MNFC with undispersed (F4_u.d.) and dispersed (F4_d.) filler, (Fig. 6).

Fig. 6 Optical and SEM images of aerogel structures of undispersed sample F4: **a–d** F4_u.d. (MNFC + undispersed) unsheared, and **e–h** F4_u.d. (MNFC + undispersed PCC) *ultralow* sheared, respectively. Regions between ice crystals where gel structure was present are easily seen in **b** and **f**. Note the large size of the voids where the crystals formed, related to the strong structure build of the system including undispersed filler. Larger magnification of sheared samples: **i** MNFC + undispersed PCC case (F4_u.d.) versus that of **j** MNFC + dispersed PCC (F4_d.)

As described earlier in the paper, freeze drying was used to remove water from the frozen samples, as described earlier by Pääkko (2008) where plastic cylinders containing the samples removed from the rheometer were dipped in liquid nitrogen and placed in the freeze dryer. After sublimation of water crystals from the frozen samples, white, light scattering, sponge-like aerogels, with a very low density, are obtained (Jin et al. 2004). This freeze drying technique did not cause complete microscopic collapse of the sample, even after shrinkage of the microstructure, as could be confirmed with optical and SEM imaging, (Fig. 6i, j).

The suspension samples were all loaded in the rheometer with constant wet starting volume. The frozen and dried gels form a structurally intact plug, but of markedly different volume depending on shear versus no shear, but retaining the total solids content. There is, thus, an evident difference in aerogel plug size, as viewed perpendicular to the cylindrical axis, between samples when comparing unsheared versus sheared, (Fig. 6a–e). In the cases where shear has been applied, and the sample has been frozen before full relaxation can occur, we see a significant porous structure build, which provides space for the ice crystals to expand, (Fig. 6e). Additionally, comparing in more detail samples that did not undergo *ultralow* shearing with those that have undergone shearing, there is a visible difference in pore size and 2D sheet-like structure between those that have undispersed filler versus dispersed filler, where the water crystal size was much larger in the case of the MNFC with undispersed filler system (F4_u.d.).

Optical and SEM images of freeze dried aerogel structures of undispersed sample without and with application of *ultralow* shear show the extent to which the structure has been expanded by the development of internal stress during shear. In the SEM subimages in Fig. 6b–f, we see the regions where the gel structures

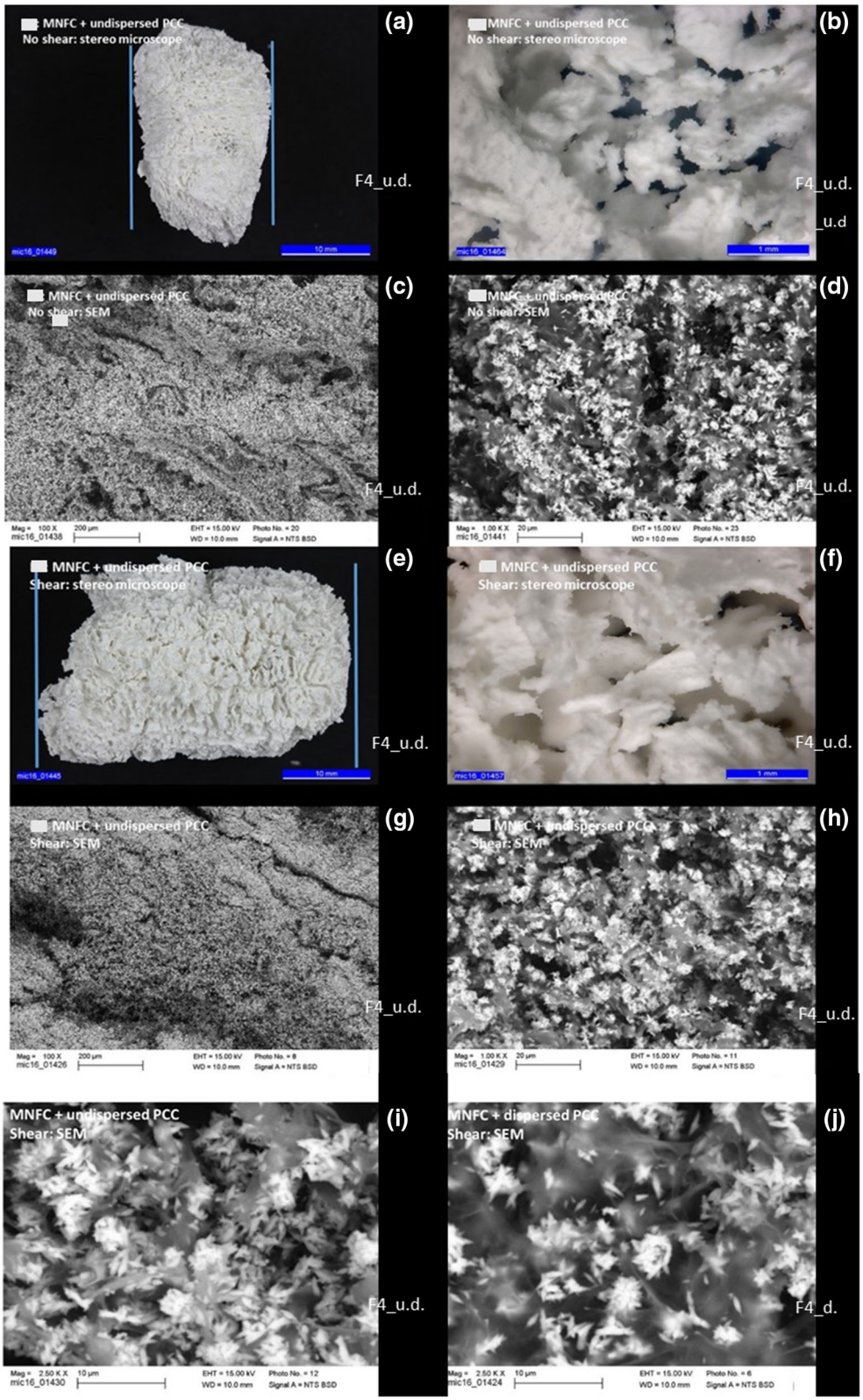
MNFC + undispersed PCC
No shear: stereo microscope
(a)
F4_u.d.
MNFC + undispersed PCC
No shear: stereo microscope
(b)
F4_u.d.
_u.d
MNFC + undispersed PCC
No shear: SEM
(c)
F4_u.d.
MNFC + undispersed PCC
No shear: SEM
(d)
F4_u.d.
MNFC + undispersed PCC
Shear: stereo microscope
(e)
F4_u.d.
MNFC + undispersed PCC
Shear: stereo microscope
(f)
F4_u.d.
MNFC + undispersed PCC
Shear: SEM
(g)
F4_u.d.
MNFC + undispersed PCC
Shear: SEM
(h)
F4_u.d.
MNFC + undispersed PCC
Shear: SEM
(i)
F4_u.d.
MNFC + dispersed PCC
Shear: SEM
(j)
F4_d.

were replaced by ice crystals. Here we note the large size of the voids where the crystals formed, related to the strong structure build of this system including undispersed filler (F4_u.d.). The SEM subimages in Fig. 6c, g, and Fig. 6d, h, illustrate the level of which the filler is distributed outside the continuum of the gel. The largest magnification in the series is presented showing the sheared samples in Fig. 4i MNFC/undispersed PCC (F4_u.d.), and that of Fig. 4j MNFC/dispersed PCC (F4_d.).

The imaging clearly shows the difference in floc structure, where the undispersed PCC is visibly demixed and flocculated and essentially excluded from the gel water matrix while forming the fibril flocculated structure. This effect is then responsible for the subsequent ability to induce dewatering of the sample.

Conclusion

In this work we have observed a mechanism of demixing and autoflocculation when undispersed, colloidally-unstable particles, in this case mineral pigment (PCC), are added to enzymatically pretreated micro nanofibrillated cellulose (MNFC) under conditions of *ultralow* shear, generating stress levels below the apparent yield stress. This internal phase separation within the sample separates the undispersed pigment PCC from the gel-like held water in the MNFC suspension. The mechanism results in significant dewatering of the otherwise extremely difficult to dewater gel. It is proposed that by inducing stress in this way in such multicomponent systems it is possible to initiate removal of significant volumes of free-flowing water from a low solids, otherwise strongly water-retaining, particulate suspension. Furthermore, this mechanism of releasing non-bound water via two component solids demixing and differential autoflocculation is, in principle, recyclable simply by applying a short application of higher shear before further reapplying the *ultralow* shear regime. Such recycling could be used as an extremely low energy gel dewatering process with applications across many osmotically driven systems. The potential for application in a wide range of fields of endeavour can, thus, be recognised, for example in waste water treatment, environmental water recovery, extraction of actives in pharmaceutical manufacture, concentration of gel-like suspensions, desalination etc.

This work as presented is limited to a particular type of MNFC derived from mechanical fibrillation of enzymatically treated fibre pulp. Extension to investigating the behaviour of other types of micro and nanofibrillated cellulose needs focus on the impact of fibril length, fibril aspect ratio, surface charge and enzymatic pretreatment, and this will be the subject of further work.

References

Chaari F, Racineux G, Poitou A, Chaouche M (2003) Rheological behavior of sewage sludge and strain-induced dewatering. Rheol Acta 42:273–279

Dalpke B, Kerekes RJ (2005) The influence of fibre properties on the apparent yield stress of flocculated pulp suspensions. J Pulp Pap Sci 31:39–43

Dentel SK, Abu-Orf MM, Walker CA (2000) Optimization of slurry flocculation and dewatering based on electrokinetic and rheological phenomena. Chem Eng J 801:65–72

Dimic-Misic K, Puisto A, Paltakari J, Alava M, Maloney TC (2013a) The influence of shear on the dewatering of high consistency nanofibrillated cellulose furnishes. Cellulose 20:1853–1864

Dimic-Misic K, Puisto A, Gane PAC, Nieminen K, Alava M, Paltakari J, Maloney TC (2013b) The role of MFC/NFC swelling in the rheological behavior and dewatering of high consistency furnishes. Cellulose 20:2847–2861

Dimic-Misic K, Nieminen K, Gane PAC, Maloney TC, Sixta H, Paltakari J (2014) Deriving a process viscosity for complex particulate nanofibrillar cellulose gel-containing suspensions. Appl Rheol 24:13653

Dimic-Misic K, Hummel M, Paltakari J, Sixta H, Maloney TC, Gane PAC (2015a) From colloidal spheres to nanofibrils: extensional flow properties of mineral pigment and mixtures with micro and nanofibrils under progressive double layer suppression. J Colloid Interface Sci 446:31–43

Dimic-Misic K, Maloney TC, Gane PAC (2015b) Defining a strain-induced time constant for oriented low shear-induced structuring in high consistency MFC/NFC-filler composite suspensions. J Appl Polym Sci. doi:10.1002/APP.42827

Dimic-Misic K, Rantanen J, Maloney TC, Gane PAC (2016) Gel structure phase behavior in micro nanofibrillated cellulose containing in situ precipitated calcium carbonate. J Appl Polym Sci 132:42827–42840

Fall AB, Lindström SB, Sundman O, Ödberg L, Wågberg L (2011) Colloidal stability of aqueous nanofibrillated cellulose dispersions. Langmuir 27:11332–11338

Haavisto S, Koponen AI, Salmela J (2014) New insight into rheology and flow properties of complex fluids with Doppler optical coherence tomography. Front Chem. doi:10.3389/fchem.2014.00027

Habibi Y (2014) Key advances in the chemical modification of nanocelluloses. Chem Soc Reviews 43(5):1519–1542

Henriksson M, Henriksson G, Berglund LA, Lindström T (2007) An environmentally friendly method for enzyme-assisted preparation of microfibrillated cellulose (MFC) nanofibers. Eur Polym J 43:3434–3441

Hogg R (2000) Flocculation and dewatering. Int J Miner Process 58:223–236

Horvath AE, Lindström T (2007) The influence of colloidal interactions on fiber network strength. J Colloid Interface Sci 309:511–517

Jin H, Nishiyama Y, Wada M, Kuga S (2004) Nanofibrillar cellulose aerogels. Colloids Surf A Physicochem Eng Asp 240:63–67

Karppinen A, Vesterinen AH, Saarinen T, Pietikäinen P, Seppälä J (2011) Effect of cationic polymethacrylates on the rheology and flocculation of microfibrillated cellulose. Cellulose 18:1381–1390

Klemm D, Kramer F, Moritz S, Lindström T, Ankerfors M, Gra D, Dorris A (2011) Nanocelluloses: a new family of nature-based materials. Angew Chem Int Ed 5024:5438–5466

Liimatainen H, Visanko M, Sirviö J, Hormi O, Niinimäki J (2013) Sulfonated cellulose nanofibrils obtained from wood pulp through regioselective oxidative bisulfite pretreatment. Cellulose 20:741–749

Martoïa F, Perge C, Dumont PJ, Orgéas L, Fardin MA, Manneville S, Belgacem MN (2015) Heterogeneous flow kinematics of cellulose nanofibril suspensions under shear. Soft Matter 11:4742–4755

Mikkelsen LH, Mascarenhas T, Nielsen PH (2002) Key parameters in sludge dewatering: testing for the shear sensitivity and EPS content. Water Sci Technol 46:105–114

Mohtaschemi M, Dimic-Misic K, Puisto A, Korhonen M, Maloney T, Paltakari J, Alava MJ (2014) Rheological characterization of fibrillated cellulose suspensions via bucket vane viscometer. Cellulose 21:1305–1312

Naderi A, Lindström T (2014) Carboxymethylated nanofibrillated cellulose: effect of monovalent electrolytes on the rheological properties. Cellulose 21:3507–3514

Naderi A, Lindström T (2015) Rheological measurements on nanofibrillated cellulose systems: a science in progress. Nova Science Publishers Inc, New York, pp 187–202

Nazari B, Moghaddam RH, Bousfield D (2013) A three dimensional model of a vane rheometer. Int J Heat Fluid Flow 42:289–295

Nazari B, Kumar V, Bousfield WD, Toivakka M (2016) Rheology of cellulose nanofibers suspensions: boundary driven flow. J Rheol 60:1151

Nechyporchuk O, Belgacem MN, Pignon F (2014) Rheological properties of micro-/nanofibrillated cellulose suspensions: wall-slip and shear banding phenomena. Carbohydr Polym 112:432–439

Nechyporchuk O, Belgacem MN, Pignon F (2016) Current progress in rheology of cellulose nanofibril suspensions. Biomacromolecules 17:2311–2320

Osong SH, Norgren S, Engstrand P (2015) Processing of wood-based microfibrillated cellulose and nanofibrillated cellulose, and applications relating to papermaking: a review. Cellulose 23:93–123

Pääkkö M, Vapaavuori J, Silvennoinen R, Kosonen H, Ankerfors M, Lindström T, Berglund LA, Ikkala O (2008) Long and entangled native cellulose I nanofibers allow flexible aerogels and hierarchically porous templates for functionalities. Soft Matter 4:2492–2499

Puisto A, Illa X, Mohtaschemi M, Alava M (2012) Modeling the rheology of nanocellulose suspensions. Nord Pulp Pap Res J 27:277

Rantanen J, Dimic-Misic K, Kuusisto J, Maloney TC (2015) The effect of micro and nanofibrillated cellulose water uptake on high filler content composite paper properties and furnish dewatering. Cellulose 22:4003–4015

Roussel N, Lanos C (2004) Particle fluid separation in shear flow of dense suspensions: experimental measurements on squeezed clay pastes. Appl Rheol 14:256–265

Saarinen T, Lille M, Seppälä J (2009) Technical aspects on rheological characterization of microfibrillar cellulose water suspensions. Annu Trans Nord Rheol Soc 17:121–128

Saarikoski E, Saarinen T, Salmela J, Seppälä J (2012) Flocculated flow of microfibrillated cellulose water suspensions: an imaging approach for characterisation of rheological behaviour. Cellulose 19(3):647–659

Saito T, Nishiyama Y, Putaux JL, Vignon M, Isogai A (2006) Homogeneous suspensions of individualized microfibrils from TEMPO-catalyzed oxidation of native cellulose. Biomacromolecules 7:1687–1691

Schenker M, Schoelkopf J, Mangin P, Gane PAC (2015) Pigmented micro-nanofibrillated cellulose (MNFC) as packaging composite material: a first assessment. In: Proceedings of the Tappi PaperCon '15 Conference, Atlanta, Tappi Press, Atlanta

Schenker M, Schoelkopf J, Mangin P, Gane P (2016) Rheological investigation of complex micro and nanofibrillated cellulose (MNFC) suspensions: discussion of flow curves and gel stability. Tappi J 15:405–416

Serra T, Casamitjana X (1998) Structure of the aggregates during the process of aggregation and breakup under a shear flow. J colloid interface sci 206(2):505–511

Spence KL, Venditti RA, Rojas OJ, Habibi Y, Pawlak JJ (2011) A comparative study of energy consumption and physical properties of microfibrillated cellulose produced by different processing methods. Cellulose 18(4):1097–1111

Spicer PT, Pratsinis SE, Raper J, Amal R, Bushell G, Meesters G (1998) Effect of shear schedule on particle size, density, and structure during flocculation in stirred tanks. Powder Technol 97(1):26–34

Tiller FM, Yeh CS, Tsai CD, Chen W (1987) Generalised approach to thickening, filtration, and centrifugation. Filtr separation 24(2):121–126

Unno H, Huang X, Akehata T, Hirasa O (1991) Gel dewatering process for biological slurry. Polymer Gels. Springer, US, pp 183–192

Wågberg L, Decher G, Norgren M, Lindström T, Ankerfors M, Axnäs K (2008) The build-up of polyelectrolyte multilayers of microfibrillated cellulose and cationic polyelectrolytes. Langmuir 24:784–795